ADVANCED MATERIALS

Raman Scattering in High-T_c Superconductors**

By Christian Thomsen*

1. Introduction

Raman scattering has yielded a wealth of information about the fascinating new high-T_c superconductors. On the one hand, many material aspects may now be analyzed non-destructively, quicker and with higher sensitivity than with conventional techniques; on the other hand, a number of fundamental properties have been examined, the most important ones to date being a value of the superconducting energy gap 2Δ and an estimate of the Fermi velocity in $YBa_2Cu_3O_{7-\delta}$. Both of these quantities are determined via the coupling of the electronic system to the phonons which are actually measured in Raman scattering. The scattering of light in these substances is, however, not limited to the study of phonons; collective magnetic excitations (magnons) have been analyzed in $YBa_2Cu_3O_6$ and there is also a poorly understood signature of scattering of electronic excitations in the superconductor.

In this article I review both the material-characterization aspects as well as some of the new physical insight Raman scattering has given us into the electron–phonon coupling in these superconductors.

2. Experimental Procedure

Experimentally, Raman scattering has the advantage that state-of-the-art instruments may be bought as turn-key systems. Due to the small penetration depth of visible light in metals in general and in the superconductors in particular (~ 500 Å), the scattering volume and hence the Raman signals are very small. Compared to the well-known peak of the optical phonon in crystalline Si, the peak of the strongest signal in $YBa_2Cu_3O_{7-\delta}$ is reduced by a factor of 50 (for excitation with a laser energy of ~ 2.4 eV). A short turn-around time in the experiment is thus achieved only by multichannel detectors such as charge-coupled devices (CCD) which are readily available. For the measurements presented in this article, I have used a Dilor XY triple spectrometer with a Photometrics CCD attached. The laser power used in the experiments on high-T_c materials must be kept comparatively low to avoid serious heating effects. Typically, in a room-temperature experiment, ~ 20 mW may be focused with a spherical lens onto a ~ 50 μm diameter spot on the sample surface without inducing irreversible damage such as oxygen loss in $YBa_2Cu_3O_{7-\delta}$. For the low-temperature experiments, which I will describe below, only about 5–10 times less power is allowed. Raman microscopes with cryostages are available and allow a lateral spatial resolution of ~ 2 μm, an advantage in analyzing microstructures or multicomponent samples.

A typical measurement of a sample may look like this: The sample is fixed on a mount, the incident laser beam focused on the sample surface, the scattered light dispersed by a monochromator, collected for 10–100 min, and the detector read out by a computer. Depending on the particular objective of a measurement, the experiment may be repeated with different polarizations of incident and scattered light, at different temperatures, with different laser wavelengths or by varying the sample orientation or composition. The unit of energy usually plotted in Raman spectra is wavenumbers in cm^{-1}. Although it would appear more sensible in solid-state physics to use meV (1 meV = 8.065 cm^{-1}), the usage of wavenumbers has traditional reasons and since traditions are strong, I will stick mostly to the latter.

3. Principles of Raman Scattering in Solids

A series of books has been devoted to light scattering in solids[1] covering in detail many aspects of Raman scattering. For the purpose of this article, however, it is sufficient to know the following: The scattered electric field ($\vec{E}_s$) is related to the incident electric field ($\vec{E}_L$) via the Raman tensor $\ddot{R}$. The experimentally determined Raman intensity I is given by Equation 1:

$$I \sim |\vec{E}_s \cdot \ddot{R} \cdot \vec{E}_L|^2 \quad (1)$$

It is for most purposes sufficient to be aware of the proportionality; absolute scattering cross sections are rarely measured, although a theory of Raman scattering in a particular material should, of course, be able to account also for the absolute magnitude of the observed signals. When the excitation wavelength is changed, care must be taken to normalize the instrumental response for the different laser energies before comparing the various spectra with one another.

[*] Dr. C. Thomsen
Max-Planck-Institut für Festkörperforschung
Heisenbergstrasse 1, W-7000 Stuttgart 80 (FRG)

[**] I thank my collaborators at the Max-Planck-Institut in Stuttgart and in particular M. Cardona for a critical reading of this manuscript and B. Friedl and V. Hadjiev for providing some of the data used in this article. The work was supported in part by the Bundesminister für Forschung und Technologie and the European Community. [AM R113]

The possible Raman tensors of a compound are characteristic for the crystallographic point group and the occupied sites of the crystal. The Raman tensor of a particular vibration, for example, has the same symmetry as the corresponding vibrational displacements in the unit cell. It follows from this that once the crystallographic point group and the occupied site symmetries of a compound are known, the Raman tensors of the Raman-active eigenvibrations may be derived. One convenient way of performing this group-theoretical analysis is using the tables of Rousseau et al.[2] For the high-T_c materials this has been done many times by now; the interested reader may consult the literature.[3] For $YBa_2Cu_3O_{7-\delta}$, which is in the orthorhombic space group D_{2h}^1, it suffices here to say that five Raman-active vibrational modes have A_g symmetry (i.e., are fully symmetric), five have B_{2g}, and five B_{3g} symmetry. The five vibrations of A_g symmetry belong to displacements of the apex-oxygen, of the two oxygen atoms in the CuO_2 plane, of Cu and Ba in descending order in frequency. Experimentally, it turns out that the A_g phonon peaks are strongest, the B_{2g}, B_{3g} modes being 10 to 100 times weaker. A typical spectrum is shown in Figure 1, where yttrium in $YBa_2Cu_3O_7$ has been replaced by Dy. It is

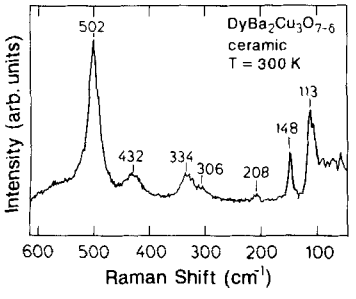

Fig. 1. Raman spectrum of a $DyBa_2Cu_3O_{7-\delta}$ ($\delta \approx 0$) ceramic. The three highest-frequency peaks correspond to oxygen A_g vibrations, the two lowest ones to vibrations of Cu (148 cm^{-1}) and Ba (113 cm^{-1}). The modes at 208 and 306 cm^{-1} correspond to B_{2g} and B_{3g} vibrations of the apex-oxygen atoms.

well known that with the exception of Ce, Pr, and Tb any rare-earth element 'R' can be substituted for yttrium without affecting the superconducting properties significantly. The Raman frequencies shift somewhat, mainly due to changes in the lattice constants. For the remainder of this article I will ignore the $B_{2g,3g}$ modes.

$$\begin{pmatrix} a & & \\ & b & \\ & & c \end{pmatrix} \tag{2}$$

The Raman tensor of an A_g mode in the orthorhombic point group (D_{2h}) is as shown in Equation 2 where the zeros in the matrix are not given. In most high-T_c materials one can make the following approximation: Since the high-T_c superconductors may be considered as slightly distorted tetragonal structures, the Raman tensors have nearly tetragonal symmetry ($a \approx b$). Then, the fully symmetrical modes of the orthorhombic group [Eqn. (2)] can be represented as shown in Equations 3 or 4.

$$\begin{pmatrix} a & & \\ & a & \\ & & c \end{pmatrix} \tag{3}$$

$$\begin{pmatrix} a & & \\ & -a & \\ & & 0 \end{pmatrix} \tag{4}$$

The first tensor is fully symmetrical in the tetragonal point group (D_{4h}) and labeled A_{1g}; the second is not fully symmetrical and has B_{1g} symmetry. The latter symmetry occurs only once for the particular sites occupied for $YBa_2Cu_3O_{7-\delta}$. One of the A_g modes of the orthorhombic structure thus has a Raman tensor $\overleftrightarrow{R}$ which may be written as shown in Equation 5.

$$\begin{pmatrix} a+\varepsilon & & \\ & -a+\varepsilon & \\ & & \approx 0 \end{pmatrix} \quad \text{with } \varepsilon \ll 1. \tag{5}$$

$$I_{\parallel} \propto \varepsilon^2 \approx 0 \quad \text{and} \quad I_{\perp} \propto a^2 \tag{6}$$

From measurements with polarizations of the excitation light along the crystal axes $\hat{a}$ or $\hat{b}$ the sign of the particular

Christian Thomsen studied physics at the University of Tübingen. After receiving his Vordiplom, he was granted a Fulbright fellowship to study physics at the Graduate School of Brown University, Providence, Rhode Island, where he obtained an Sc.M. in both electrical engineering (1984) and physics (1985) as well as a Ph.D in physics (1986). At Brown he remained as a postdoc until 1987, working on time-resolved acoustic-phonon spectroscopy in amorphous and crystalline solids. Since 1987 he has been working at the Max-Planck-Institut für Festkörperforschung in Stuttgart in the group of Manuel Cardona, where he holds a staff position. His current research activities lie in Raman scattering in high-T_c superconductors and the investigation of electron-phonon coupling in these materials. He completed his habilitation at the Technical University of München in 1991. Also in 1991 he received the Walter-Schottky-Prize for his contributions to the understanding of high-T_c superconductivity.

© VCH Verlagsgesellschaft mbH, W-6940 Weinheim, 1992 0935-9648/92/0505-0342 $ 3.50+.25/0 Adv. Mater. 4 (1992) No. 5

ADVANCED MATERIALS

tensor element is not distinguishable, but for polarizations along the diagonals [110] or [1$\bar{1}$0] Equation 6 can be derived from Equations 1 and 5, where $\parallel$ refers to parallel and $\perp$ to perpendicular relative polarizations of incident and scattered light. The peculiarity of this mode is such that it may be singled out from the other four A_g modes by its polarization properties alone. In the literature, it is often referred to as the B_{1g}-like mode, and it has special importance since its frequency ($\sim 340\ cm^{-1}$ or 42 meV in $YBa_2Cu_3O_{7-\delta}$) lies near the superconducting energy gap and this vibration reacts particularly sensitively to the superconducting phase transition.

4. Characterization of High-T_c Samples

A number of characteristics of a sample may be obtained from what we have presented so far.

- Its composition:

Since secondary phases present in a sample have in general a different crystal symmetry, they also have different Raman tensors and frequencies. The commonly occurring "green phase" R_2BaCuO_5 for example, has a Raman spectrum as shown in Figure 2 (For 'R' = Tm), clearly distinct from the

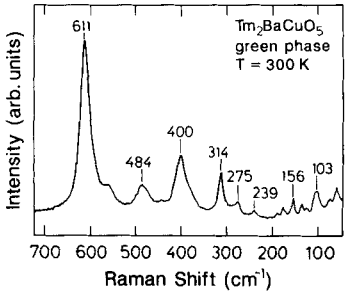

Fig. 2. Raman spectrum of the so-called green phase R_2BaCuO_5 (here R = Tm), a commonly occurring secondary phase in the preparation of $RBa_2Cu_3O_7$. The characteristic peak at 611 cm^{-1} is easily recognized if the green phase is present in a sample of the superconductor. For other 'R', the frequency at this peak may be slightly different (e.g. 'R' = Y, 600 cm^{-1}).

Raman spectrum of a clean $RBa_2Cu_3O_7$ (R = Dy) sample (Fig. 1). $BaCuO_{2-n}$ has a spectrum as shown in Figure 3 and is present in samples prepared with Ba excess. The intensity and frequency of the peak at 630 cm^{-1} (78 meV) may vary somewhat depending on the oxygen content. The sensitivity of Raman scattering to these secondary phases is quite high because they are usually insulators and hence less absorbing. For equal excitation-laser intensity and ceramic samples, the Raman signal of the 600 cm^{-1} (74 meV) peak of the "green phase" is $\sim$30 times stronger than that of the 580 cm^{-1} (72 meV) peak in $BaCuO_2$, and $\sim$6 times stronger than the 500 cm^{-1} (62 meV) peak in the superconductors. Thus the Raman method can detect as little as $\sim$0.2% "green phase" and $\sim$1% of $BaCuO_2$ averaged over the area illuminated by the laser spot. It is clear, though, that phases which are not Raman active cannot be detected.

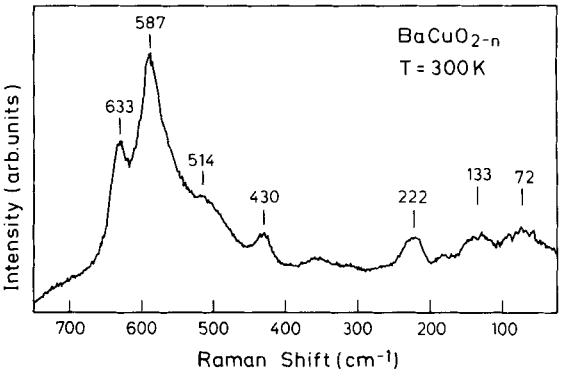

Fig. 3. Spectrum of $BaCuO_2$, a common secondary phase when preparing $RBa_2Cu_3O_7$.

- Orientation:

From the tensorial origin of the Raman signal it is possible to determine the crystal axes. The mode at 500 cm^{-1} (61.8 meV) in $YBa_2Cu_3O_7$ has A_g symmetry; experimentally it turns out that the tensor component c in Equation 3 is much larger than a ($c \gg a$). Thus we may judge from the strength of this line in the spectrum how much c-axis component is in the investigated sample surface. Another peak, the one at 340 cm^{-1} (42 meV), has $c \approx 0$ (Eq. 5) and, for a sample fully oriented with $\vec{E}_L \parallel \vec{E}_s \parallel \hat{c}$, this peak should not be present. Figures 4 and 5 demonstrate the difference in orientation on a thin-film sample. The spectra are of a film which

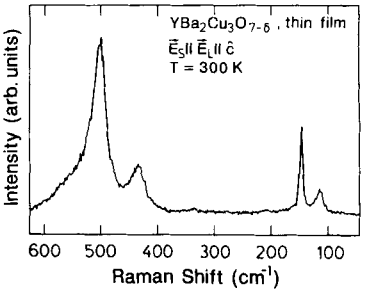

Fig. 4. Spectrum of an oriented thin film of $YBa_2Cu_3O_{7-\delta}$ ($\delta \approx 0$). The c-axis is in the plane of the substrate and incident and scattered light are parallel to $\hat{c}$.

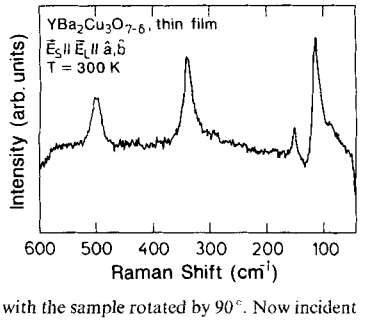

Fig. 5. Same film as in Fig. 4 but with the sample rotated by 90°. Now incident and scattered electric fields are in the ab-plane.

  0935-9648/92/0505-0343 $ 3.50+.25/0

has the c-axis oriented in the plane of the substrate. Figure 4 shows the spectrum for $\vec{E}_L \parallel \vec{E}_s \parallel \hat{c}$, as can be judged from the absence of the mode at 340 cm^{-1} and the strength of the 500 cm^{-1} mode. Figure 5 shows the spectrum after rotation of the sample by 90°; now $\vec{E}_L \parallel \vec{E}_s \parallel \hat{a}, \hat{b}$, the 340 cm^{-1} mode is present, and the high-energy and at 500 cm^{-1} has become much weaker.

In a similar way, a and b-axes of untwinned specimens may be distinguished: the a-component in Equation 2 of the mode at 115 cm^{-1}(14.3 meV) is smaller than the a-component of the 340 cm^{-1} mode. The b-components are nearly equal. Figure 6 clearly shows the described effect in the Raman spectra of an untwinned single crystal of $YBa_2Cu_3O_7$. The upper curve is taken with electric fields parallel to the a-axis, the lower one with those parallel to the b-axis. The

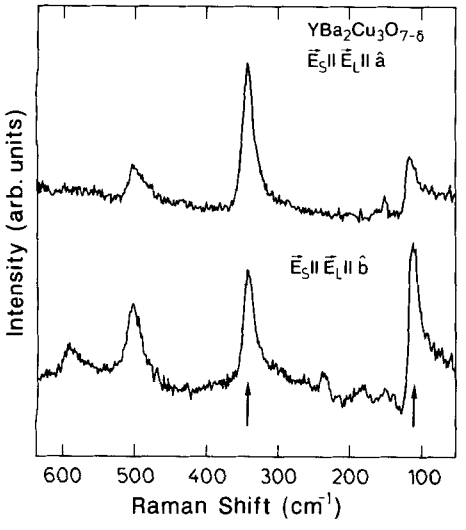

Fig. 6. Raman spectra on untwinned single crystals allow the distinction between $\hat{a}$ and $\hat{b}$ axes of the crystal from the relative difference in the amplitude of the peaks at 115 cm^{-1} and 340 cm^{-1}.

additional peaks at 230 and 580 cm^{-1} (28 and 72 meV) which appear only in the lower curve are characteristic of ordering defects in the CuO chains. They are absent in well-annealed thin films or ceramic samples. Since these orientational properties may be checked under an optical microscope, Raman scattering may in some instances provide more useful information than X-ray diffraction.

- Impurities and Defects:

Impurities and defects in the crystal structure may also be checked for with Raman spectroscopy. The oxygen concentration, which determines the superconducting properties of $YBa_2Cu_3O_{7-\delta}$, is in a roughly linear relationship with the frequency of the mode at 500 cm^{-1}. For the semiconductor ($\delta \approx 1$) the frequency is 475 cm^{-1} (59 meV) and, once calibrated, the actual frequency of this mode in a given sample is an accurate, non-destructive way of determining the oxygen concentration.[3]

Other impurities such as heavy-metal ions are harder to check for. As an example, recently, the presence of gold in the formula $YBa_2Cu_{3-x}Au_xO_{7-\delta}$ was demonstrated by examining the temperature dependence of the linewidth and frequency of the 340 cm^{-1} mode for different Au concentrations. Leaving the discussion of why the linewidth reacts so sensitively to the superconducting state for later, we clearly see a dependence of the low-temperature behavior on Au concentration.[4] Also, in the normal state (say at room temperature) the linewidth of the phonons depends in general on the impurity concentration and, once suitably calibrated, may be used for an estimate. It turns out that many impurities have a similar effect, so that once the type of impurity is known, a curve as in Figure 7 may show how much impurity a particular sample contains. Alternatively, given that absolute linewidths of some phonons depend on the impurity concentration, the width may be used for this purpose.

- Microstructure Analysis:

With the microscopic resolution of a Raman system, it becomes possible to laterally analyze microstructures. Com-

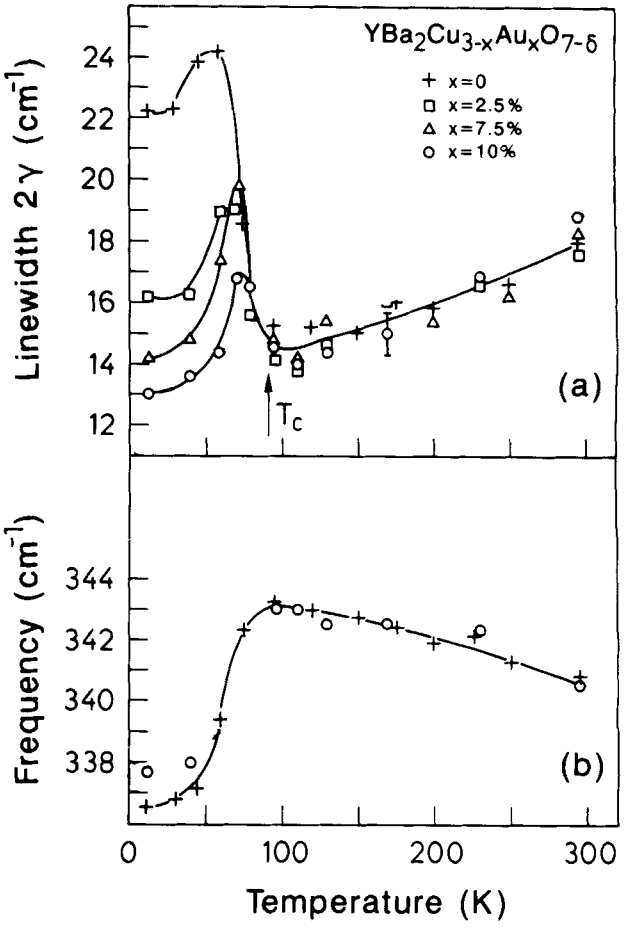

Fig. 7. Temperature dependence of the Raman frequencies and linewidths of various gold-containing samples of $YBa_2Cu_{3-x}Au_xO_{7-\delta}$. While the frequencies are not affected very much, the linewidth broadening in the superconducting state depends on Au concentration and may be used to estimate x in an actual sample. Such a contamination may occur in crystals grown in a gold crucible.

0935-9648/92/0505-0344 $ 3.50+.25/0

ADVANCED MATERIALS

mercially available automatic x–y positioning tables and a computer-controlled readout of data as well as two-dimensional detectors may be of help in such an analysis.

5. Fundamental Physical Properties of $YBa_2Cu_3O_{7-\delta}$

Many important physical properties of the high-temperature superconductors have been determined by Raman scattering. Some of the more recent highlights in this field will now be presented. Of utmost interest is the realization that through the behavior of the phonons seen in the Raman spectra it is possible to determine a value of the superconducting gap.[5] Here, one takes advantage of the fact that through electron–phonon coupling the phonons feel the opening of the gap as a change in the electronic density of states. The effect is clearest near the value of the gap, in $YBa_2Cu_3O_{7-\delta}$ $2\Delta(0) = 320\ cm^{-1}$ (=40 meV), which is why the phonon at 340 cm^{-1} (42 meV) is affected most. Figure 8 shows the linewidth changes of this phonon between the superconducting and normal state, where the absolute frequency has been shifted by replacing Y with various rare-earth elements.

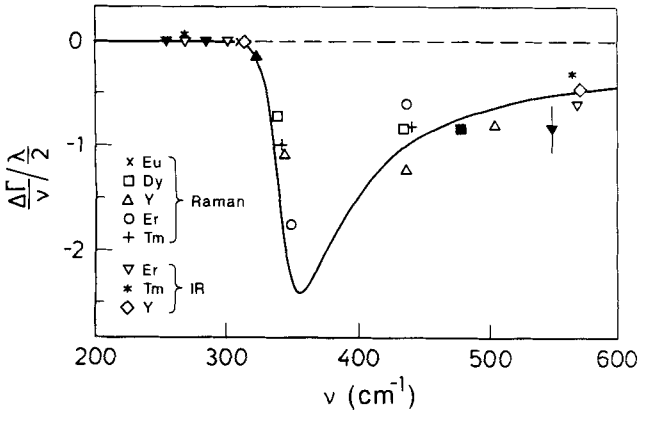

Fig. 8. Phonon-linewidth changes between superconducting and normal state of $RBa_2Cu_3O_{7-\delta}$. The experimentally determined values, normalized by the absolute phonon frequency, and the electron–phonon coupling constant λ of the phonon are plotted. The onset of broadening at ~320 cm^{-1} (=40 meV) determines a value for the superconducting gap. Also included in this figure are changes in linewidth observed for infrared-active phonons.

Below a certain critical frequency, the linewidth does not increase in the superconducting state; above it, a broadening of the Raman lines sets in when the sample is cooled below T_c. Physically speaking, if a phonon in the superconducting state has an energy larger than the energy gap it can decay by breaking a Cooper pair. This causes the observed broadening and hence determines the gap value at 320 cm^{-1}. The curve drawn through the data points corresponds to a calculation by Zeyher and Zwicknagl[6] in a strong-coupling model and agrees well with the data.

Another point of interest is the coupling constant of the various phonons. Those determined at $\vec{k} = 0$ from the experiments described above correspond to a parameter $\lambda \sim 0.4$–0.8 if all phonons had the same contribution to λ. This λ is apparently too small to account for the high transition temperatures in these materials. On the other hand, the contribution of all phonons to λ is not necessarily the same. In fact, some recent evidence indicates that at the zone boundary and at special points in the Brillouin zone (so-called nesting points) the coupling may be significantly larger than in the zone center.

It is also possible to obtain information about the symmetry of the gap in $YBa_2Cu_3O_7$. In Figure 7 the effect of gold on the linewidth in the superconducting state, and how it is possible to determine the Au concentration from such a measurement is demonstrated. Why does this type of analysis work? I suggest the following way of looking at the problem: In a gold-free sample, the self-energy effects discussed above allow the determination of a gap value. The gap in these layered superconductors is, however, anisotropic, which may be intuitively clear from the anisotropic structure or various anisotropic electronic properties. This implies that the material is more in the clean limit than in the dirty limit, where such an anisotropy would not be felt so strongly. If we use the de-Gennes criterion at $T = 100$ K to estimate where the clean limit begins (Eq. 7) we find $l_{crit} = 9$ nm, where we have used a Fermi-velocity $v_F = 7.5 \times 10^7$ cm sec^{-1}.

$$l_{crit} = \frac{\hbar v_F}{2\pi k_B T} = \frac{910\ \text{nm K}}{T} \tag{7}$$

The average Au–Au distance perpendicular to the c-axis, however, for a sample with formula unit $YBa_2Cu_{3-x}Au_xO_{7-\delta}$ ($x = 0.1$), is ≈ 1.2 nm as estimated if we know that Au occupies only the chain-copper site. The introduction of these fairly high concentrations of impurity atoms puts the superconductor into the dirty limit and symmetrizes the gap. Such a symmetrization implies that a particular gap value determined by some method may change and this is what Figure 7 shows. The superconductivity-induced broadenings disappear, making it seem that the gap has moved *up* in energy. In the picture of the anisotropic gap, this implies that in the clean limit ($x = 0$) the gap determined by the phonon method corresponds to a local minimum.

Recently, it has been possible to determine the Fermi velocity in the normal state of $YBa_2Cu_3O_7$ through a Raman-scattering experiment. The main idea of the experiment is to study the wavevector-dependent decay into single-electron excitations, the so-called Landau damping.[7] Here, the goal is to detect a sudden broadening of some Raman-active phonons where the wavevector $\vec{q}$ increases to such an extent that momentum- and energy conservation laws allow a decay into the single-particle continuum. This was found to be possible for the low-frequency phonons at 115 cm^{-1} (14.3 meV) and 150 cm^{-1} (18.6 meV) for standard laser

  0935-9648/92/0505-0345 $ 3.50+.25/0

wavelengths with which we varied $\vec{q}$. For the high-frequency phonons [$\omega > 300\ cm^{-1}$ ($=37$ meV)] $\vec{q}$ with optical lasers is no longer large enough to reach the Landau-damping region and the linewidth remains independent of $\vec{q}$. The Fermi velocity determined this way is $v_F = (7.5 \pm 2.5) \times 10^7\ cm\,sec^{-1}$, the value used in the above estimate of the mean-free path of the electrons. This value corresponds to the maximum Fermi velocity of bands to which an electron–phonon coupling exists and agrees also with band-structure calculations, indicating that strong renormalization effects do not appear do take place even near the Fermi surface.

Other experiments on the high-T_c materials include resonance Raman scattering which checks the band-structure calculations obtained in the local-density approximation. Extensive studies have shown that for the most part the agreement between experiment and theory is good.[8] Another type of fundamental physics not involving superconductivity was studied by Raman scattering when the mixed state of a phonon and a crystal-field excitation was discovered in $NdBa_2Cu_3O_7$. Due to coincidences in symmetry and energy, a crystal-field level in $NdBa_2Cu_3O_7$ was found to mix with the usually observed phonons on the basis of the characteristic temperature dependences of the Raman intensities. Even more convincing evidence came from an isotope-replacement experiment where regular ^{16}O was exchanged by ^{18}O. The shift normally found from such a substitution, for example in $YBa_2Cu_3O_7$, corresponds to 6%. In the case of $NdBa_2Cu_3O_7$, due to the approximately 50% mixing of the two types of excitations,[9] however, both the phonon and the crystal-field peak shifted only by 3%.

6. Conclusions

Raman scattering has developed into a very powerful tool in the field of high-T_c superconductivity, providing information on the fundamental physical properties of the superconducting materials which other techniques could not have yielded so easily. In an industrial environment these studies could be useful for the fast and non-destructive evaluation of samples; research institutes, on the other hand, may achieve more fundamental results leading towards a solution of the high-T_c puzzle.

Received: October 15, 1991

[1] *Light Scattering in Solids I–VI* (Ed. M. Cardona, G. Güntherodt) Volumes in Applied Physics, Springer-Verlag, Berlin **1975–1991**.
[2] D. L. Rousseau, R. P. Bauman, S. P. S. Porto, *J. Raman Spectr.* **1981**, *10*, 253.
[3] see e.g. C. Thomsen, M. Cardona, in *Physical Properties of High Temperature Superconductors I* (Ed. D. M. Ginsberg) World Scientific Publ., Singapore **1989**, p. 409.
[4] C. Thomsen, B. Friedl, M. Cieplak, M. Cardona, *Solid State Commun.* **1991**, *78*, 727.
[5] B. Friedl, C. Thomsen, M. Cardona, *Phys. Rev. Lett.* **1990**, *65*, 915.
[6] R. Zeyher, G. Zwicknagl, *Z. Phys. B – Condensed Matter* **1990**, *78*, 175.
[7] B. Friedl, C. Thomsen, H.-U. Habermeier, M. Cardona, *Solid State Commun.* **1992**, *81*, 989.
[8] E. T. Heyen, S. N. Rashkeev, I. I. Mazin, O. K. Andersen, R. Liu, M. Cardona, O. Jepsen, *Phys. Rev. Lett.* **1990**, *65*, 3048.
[9] E. T. Heyen, R. Wegerer, M. Cardona, *Phys. Rev. Lett.* **1991**, *67*, 144.

0935-9648/92/0505-0346 $ 3.50+.25/0